Synthesis and Grafting Ability of Silane-Terminated Polyethylenes on Silica Surfaces

J. DUCHET,[1] J.-P. CHAPEL,[1] B. CHABERT,[1] R. SPITZ,[2] J.-F. GÉRARD[3]

[1] Laboratoire des Matières Plastiques et Biomatériaux UMR CNRS No. 5627, Université Claude Bernard Lyon I, Bât.303, 69622 Villeurbanne Cedex, France

[2] Laboratoire de Génie des Procédés de Polymérisation UMR CNRS No. 140, CPE Lyon, BP 2077, 69616 Villeurbanne Cedex, France

[3] Laboratoire des Matériaux Macromoléculaires UMR CNRS No. 5627, Institut National des Sciences Appliquées de Lyon, Bât.403, 69621 Villeurbanne Cedex, France

Received 19 July 1996; accepted 19 December 1996

ABSTRACT: Chlorosilane-terminated polyethylenes having different molar masses are prepared to be used as connecting molecules between a silica surface and a neat polyethylene matrix. The synthesis and the grafting ability of such functionalized polyethylenes is reported. The grafting efficiency is demonstrated by means of ^{29}Si NMR and wetting measurements according to the hydrophobic nature of the grafted molecules in comparison with the hydrophilic character of the silica surface. The resulting thickness and refractive index of the dry grafted layers are characterized using spectroscopic ellipsometry. The grafting ratios are given from microanalysis measurements. Surface topography is observed using AFM. All of these techniques are in a good agreement and a general trend of the organization of the tethered layers at the surface is proposed.
© 1997 John Wiley & Sons, Inc. J Appl Polym Sci **65:** 2481–2492, 1997

Key words: grafting; silica surface; silane-functionalized polyethylene surface; energy; ellispometry; atomic force microscopy

INTRODUCTION

Numerous articles were done on the interface between a semicrystalline polymer and an inorganic substrate, such as glass or carbon fibers.[1–5] In most of the cases, the interfacial phenomena in such materials was studied in terms of crystallization in the polymer in the vicinity of the inorganic surface. In fact, a transcrystalline interphase can be generated as a function of the cooling and/or shearing in the supercooled melt.[6–10] Nevertheless, most of the articles do not definitely conclude on the effect of such interfacial layer on the load transfer (i.e., the shear strength of the interface) at the interface.[11,12] Another way consists on the grafting of polymer chains on the inorganic surface.[13–16] In such a way, the polymer chains act as connecting chains between the surface and the bulk of the polymer used as matrix or coating. The improvement of the bond strength results from the entanglements of these connecting chains with the polymer chains. This concept was well described by theoretical models and verified experimentally in the case of the interface between two linear polymers connected by block copolymers.[17–20] In the case of semicrystalline polymers, the ability of the polymer chains to crystallize can be used as an additional phenomenon to increase the interfacial adhesion. In fact, if the grafted polymer chains are able to crystallize in the same crystallographic from and with the same

Correspondence to: J.-F. Gerard.
Contract grant sponsor: M.R.E.S. Minestry.

Journal of Applied Polymer Science, Vol. 65, 2481–2492 (1997)
© 1997 John Wiley & Sons, Inc. CCC 0021-8995/97/122481-12

kinetics as the "free" polymer deposited on the grafted surface, a cocrystallization between these two types of chains can be expected.[21–24] This concept was previously developed in the case of poly(phenylene sulfide)/glass[24] and isotactic polypropylene/glass interfaces.[21,22] In the later case, silane-terminated isotactic polypropylenes having different amounts of functional groups were prepared from a Ziegler–Natta polymerization and compared to silane-terminated (silane group at the end of the chain) oligopropenes.[22] The capability of such polymers to be grafted and to cocrystallize (in blends) with a neat isotactic polypropylenes was demonstrated. For the PPS/glass interface, carboxy-functionalized PPS were synthesized and the grafting on the glass surface proceed from the reaction of the carboxy functions with the amine groups of the γ-aminopropyltriethoxysilane predeposited on the glass surface forming an amide unit.[25] Large improvements of the shear strength, τ, and/or fracture energy of the interface were noted by controlling the position (as side groups or chain ends) and the amount of the functional groups and also the molar mass of the grafted chains.[26] The same type of conclusions was noted for the interface between two semicrystalline polymers, the polypropylene, and the polyamide 6-6, for which polypropylene–polyamide copolymers are formed at the interface during joining.[27] Nevertheless, the cocrystallization in the interphase region expected from the fracture energy measurements was not clearly demonstrated.

The aim of this article is to show the grafting ability of silane-terminated polyethylene on silica surface through physico-chemical characterizations of the tethered chains to verify the aptitude of such molecules to be used as connectors between a silica or glass surface and a neat polyethylene matrix. Different chlorosilane-terminated polyethylenes having different molar masses are prepared and grafted on silicon wafers with a native SiO_2 layer. The ability of such polymers to be grafted by reacting the silane group with the hydroxyl functions on the surface and the structure of the deposited polymer layer are studied by means of physico-chemical methods such as NMR, wetting, ellipsometry, and atomic force microscopy. According to the hydrophobic character of the grafted polymer and the hydrophilic character of the untreated surface, the wetting measurements can be performed to check the grafting efficiency and the structure of the grafted layer. These different methods were previously applied for grafting of short alkyl chains (alkyl dimethyl chlorosilanes $C_nH_{2n+1}—Si(CH_3)_2Cl$ with n from 4 to 30) on silica in order to determine the grafting density and the structure of the resulting layers[28]. The silane-terminated polyethylenes grafted on silica surfaces are used as connectors with a neat polyethylene matrix to enhance the polyethylene–silica interface. The study of the interfacial adhesion is reported in other articles.[29,30]

EXPERIMENTAL

Materials

The unmodified polyethylenes used in this study are produced from polymerization in heptane with a metallocene catalyst. Because all the catalysts are poisoned by air or water, all the polymerization steps are done under argon. Three kinds of polymers were prepared:

The polyethylene denoted PE-1 is a PE obtained using an homogeneous catalyst, the cyclopentadienyl zirconium dichloride (denoted Cp_2ZrCl_2) and the cocatalyst MAO (methyl aluminoxane) in a heptane solution. MAO (15 mM) followed by $1.5 \times 10^{-5} M$ of Cp_2ZrCl_2 are added to 300 mL of heptane solution. To favor the transfer reactions leading to a large decrease in the molecular mass, the polymerization takes place at high temperature, i.e., 95°C, under ethylene at low pressure (near 1 bar). The consumption of ethylene is monitored and the polymerization is stopped by a methanol addition. The polymer is then recovered by precipitation and washed in methanol.

The polyethylene denoted PE-3 is an ethylene–hexene copolymer obtained with the metallocene homogeneous catalyst, the ethenyl-bis-indenyl zirconium dichloride [denoted $Et(Ind)_2ZrCl_2$] and the cocatalyst MAO. The hexene-1 comonomer is used in this case to reduce the crystallinity of the resulting polymer and chain transfer is more frequent after an α-olefin insertion. In a 300 mL solution of heptane are brought in successively 20 mL of hexene-1, 10 mM of MAO, and just before starting the copolymerization 1.25×10^{-6} mol of $Et(Ind)_2ZrCl_2$. The reaction occurs at 65°C under a constant ethylene pressure of 4 bars. The hexene-1 being in large excess, the consumption of the comonomer is negligible, so that the reaction occurs without composition drift. The copolymer is then recovered as previously in methanol.

The PE-2 is a polyethylene obtained using an heterogeneous metallocene supported on silica (50 mg) and MAO (10 mM) as cocatalyst at 95°C.

Polymerization takes place under an ethylene pressure of 0.5 bars.

The silane functionalization of these polyethylenes is performed in xylene with chlorodimethylsilane (used as received from ABCR Products). The hydrosilylation can be described as follows:

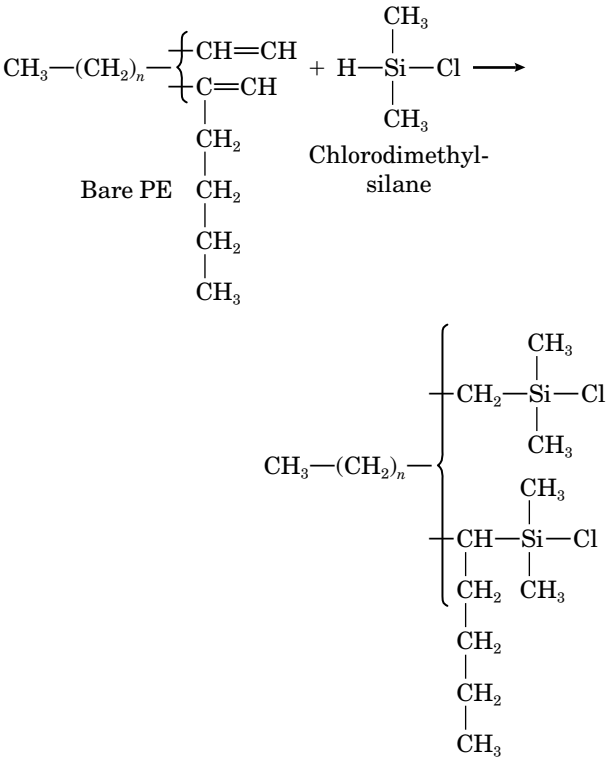

The reaction is conducted in a reactor under an argon atmosphere in dried xylene (100 : 1 for xylene-to-PE by weight) at 145°C for 2 h. A cooling to 90°C is carried out to prevent the degradation of the Speier catalyst. The catalytic solution is made from 1% (wt) of hexachloroplatinic acid (H_2PtCl_6) in isopropanol. Finally, a 2% (molar) silane in xylene (2% molar) is used for 48 h at 90°C. The polymer is then kept in solution before grafting to prevent further reactions of the chlorosilane moieties.

Table I Molar Masses of the Precursor Polyethylenes

Polymer	$\bar{M}_n$ ($g \cdot mol^{-1}$)	$\bar{M}_w$ ($g \cdot mol^{-1}$)	Ip
PE-1	1,194	5,230	4.4
PE-2	3,710	16,000	4.3
PE-3	325,000	65,000	2

Table II Melting Temperatures, T_m, and Crystalline Rates, X, of the Precursor Polyethylenes (Melting for 5 Min at 200°C and Cooling to Room Temperature at 10 $K \cdot min^{-1}$)

Polymer	T_m (°C)	X (%)
PE-1	121	49.3
PE-2	139	68.5
PE-2	91.5	17.2

Silica Surfaces

Depending on the technique of characterization used, the silane-functionalized polyethylenes are grafted on: (a) silicon wafers (30×10 mm^2) having a native SiO_2 layer and a roughness from 0.15 to 0.35 nm. The hydroxyl groups density on the surface is 4.5 nm^{-2}. (b) Pyrogenic silica particles (Aerosil 200 from Degussa) having a diameter from 7 to 12 nm and a specific area (measured by nitrogen adsorption) about 200 ± 25 $m^2 \cdot g^{-1}$. According to this high value of the specific area, the grafting density cannot easily be compared to those obtained on silicon wafers because of the size of the grafted polymer. This type of silica was considered in order to verify the ability of the PE to be chemically grafted

The cleaning and the hydroxylation of the silica substrate is a crucial step in the grafting process. The silicon wafers are cleaned by stripping off any organic contaminants by chemical and photochemical treatments. After degreasing under an ultrasonic stirring in acetone followed by an other one in methanol, the samples are brought in a quartz sealed container filled with O_2 and subject to UV light (265 nm) for 1 h. They are then dipped into a hot (110°C) H_2SO_4 : H_2O_2 solution (70 : 30 by wt) for 15 min then rinsed thoroughly with purified water. The final step involves again a 15 mn UV/ozone treatment.

The clean silica samples and a 5% solution by weight of the functionalized-PE in xylene are heated a 145°C for 2 h under an argon atmosphere. Then, these are washed with xylene in a sohxlet extractor for 5 h, dried with nitrogen, and stored for 24 h in vacuum prior any characterization. These experimental conditions were optimized in a previous study on dealing with grafted organosilanes.[28] The grafting kinetics plays obviously a key role on the structure of the tethered layer through the molecular weight distribution. A longer grafting time will lead to a thicker physisorbed layer and then a longer washing procedure without improving the chemisorbed layer.

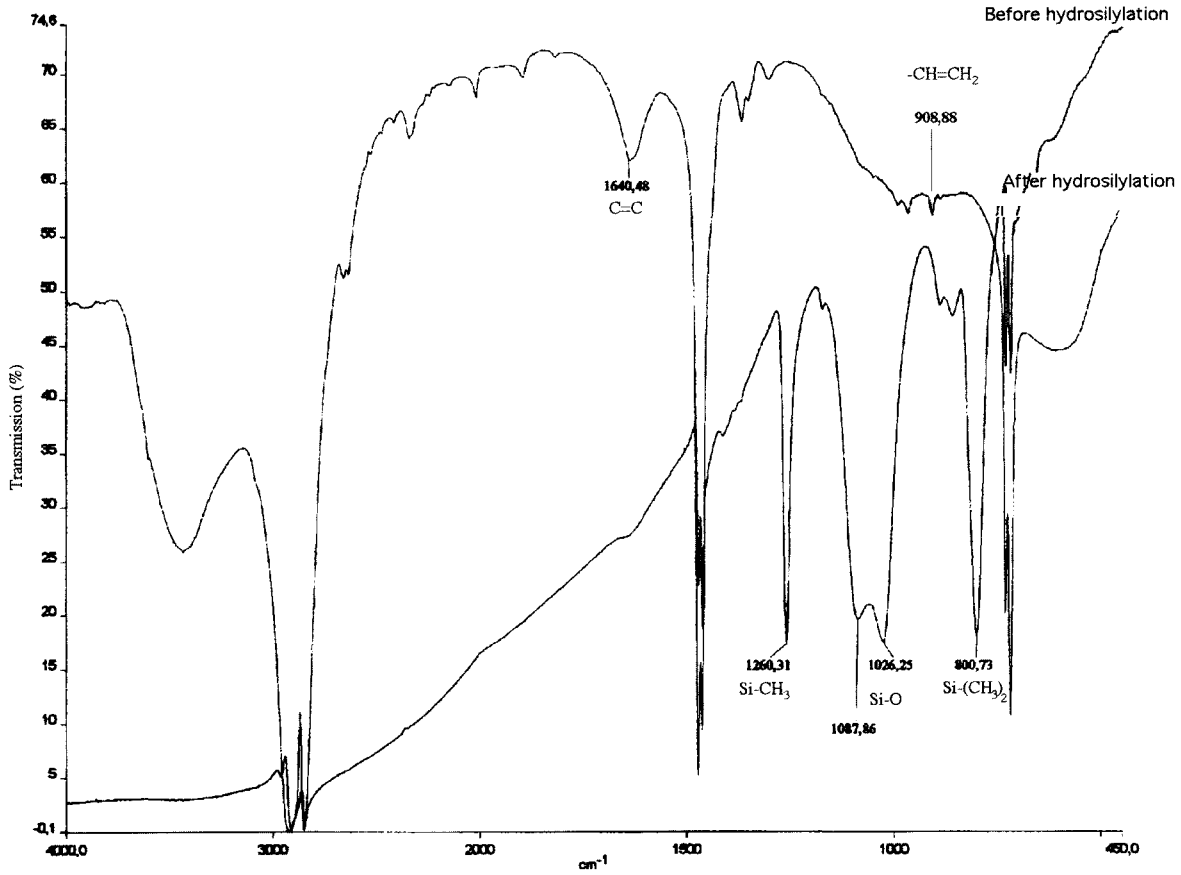

Figure 1 FT–IR spectra of the precursor polyethylene PE1 before and after hydrosylilation with chlorodimethylsilane.

Experimental Techniques

Thermograms are obtained from a Perkin–Elmer DSC7 thermal analyzer under nitrogen atmosphere on 10 mg samples. Before any measurement each sample is heated up at 200°C during 5 mn to erase their thermal history. They are then considered after have been cooled down to room temperature then heated again to 200°C at 10°C/mn. The degree of crystallinity X% is calculated using the theoretical melting enthalpy value $\Delta H_0 = 280.5\ J \cdot g^{-1}$ of a polyethylene monocrystal.

Molar mass measurements are performed on Waters-150 GPC equipped with microstyragel 10^2, 10^3, and 10^4 nm columns, after 2 h of homogenization in ortho dichlorobenzene at 135°C.

The efficiency of the hydrosilylation reaction is evaluated by transmission FT–IR spectroscopy performed using Perkin–Elmer 1760X. A drop of solution (before and after silylation is deposited onto a KBr pellet, the solvent is then removed at 145°C under vacuum.

The hydrophilic and hydrophobic wettability characteristics of respectively clean silica samples and grafted ones are measured at room temperature using the sessile drop method. A drop of a given test liquid is deposited on the silica surface. A videocamera associated with a home-made analysis device gives from the geometry of the droplet the contact angle between the liquid and the silica surface. The reported contact angle, θ, is the average value of at least 10 drops for each surface treatment of the silica surface for a given liquid. The standard deviation gives an estimation of the macroscopic homogeneity of the surface structure. The measurements are performed with

Table III Polar and Dispersive Components of the Organic Liquids Used as Probes for the Surface Energy Measurements

Liquid Probe	γ^{nd} (mN/m)	γ^{d} (mN/m)
Water	51	21.8
Diiodomethane	50.8	2.6

Table IV Wettability Measurements Performed on PE-3–Treated Silica Surfaces

	θ_{water} (°)	θ_{Diiodo} (°)	γ^d (mN/m)	γ^{nd} (mN/m)	γ (mN/m)
Wetting	102.8 ± 0.9	72.5 ± 1.1	22.5 ± 0.6	0.8 ± 0.1	23.2 ± 0.8
Dewetting	92.8 ± 1.7	63.8 ± 2.6	27.6 ± 1.5	2.0 ± 0.2	29.6 ± 1.7

distilled water in order to underline the hydrophobic character of the grafted layers. The relationships between the contact angle and the surface energy of the grafted silica is obtained by applying the generalized Fowkes theory,[31] in which the geometric average of the dispersive component of the surface free energy is extended to the polar one. For that purpose, a dispersive test liquid, the diiodomethane, is used. Measurements made with this two liquids allow us to evaluate respectively the polar γ_S^{nd} and dispersive γ_S^{d} components of the surface free energy γ through the relation:

$$\gamma_L(1 + \cos\theta) = 2\sqrt{\gamma_L^d \gamma_S^d} + 2\sqrt{\gamma_L^{nd} \gamma_S^{nd}}$$

where γ_L is the surface energy of the wetting liquid.

$$\gamma_L = \gamma^{nd} + \gamma^{d}.$$

From the atomic percentage of carbon determined on divided silica, the grafting density can be calculated using the following equation:

$$\Sigma_c = \frac{1}{A}\frac{10^6 P_c}{(1200 n_c) - P_c(M_w - 1)} \quad (\text{silane molecules}\cdot\text{nm}^{-2})$$

where A is the specific area of the bare silica, n_c is the number of carbon atoms, M_w the molar mass of the bonded moiety, and P_c the percentage of carbon for the grafted silica.

The surfaces are examined in air using a commercial AFM from Park Scientific Instrument. A laser beam strikes a cantilever and the deflection of the laser beam caused by the movement of the lever is detected with a four section photodetector. Recording the deflection of the cantilever, the local height of the sample is measured. Untreated and grafted silica are analyzed using a V-shaped Si_3N_4 microlever cantilever with a nominal spring constant of $0.58\ N\cdot mm^{-1}$ possessing a pyramidal sensor tip with a radius of curvature lower than 20 nm (the interaction zone is then a few ten of nanometer square). AFM measurements give a realistic feature of the local structure of the surface. All scans are performed in contact mode, i.e., the probe tip is moved into a continuous contact with the specimen surface and scanned over the surface with a frequency of 2 Hz. It is worth saying that from holes in the layer structure it is always possible to estimate the thickness of the grafted layer. This value, although not absolute (because we are never sure to be in contact with silica) could then be compared with more appropriate technics.

Indeed, the absolute thicknesses of the grafted layers are evaluated from ellipsometric measurements. Ellipsometry is based on the fact that a monochromatic electromagnetic wave changes its state of polarization after striking a reflecting surface. This change is a function of the optical parameters of the whole system. The relationship between these parameters and the ellipsometric measured angles can be expressed as[32]:

$$e^{i\Delta}\tan\Psi = \frac{R_p}{R_s} = f(n_k, d_k, \lambda, \phi)$$

where R_p and R_s represent the overall reflection coefficients for the basis p- and s-waves, respectively. They are dependent on n_k and d_k, which refer the refraction index and the thickness of each layer of the model (Fig. 2), λ is the wavelength, and ϕ is the angle of incidence. Measurements of Δ and Ψ allow the evaluation of the two unknown parameters, the polymer layer thickness, and its refractive index.

In this work, measurements are performed at

Table V Wettability Measurements Performed on PE-2–Treated Silica Surfaces

	θ_{water} (°)	θ_{Diiodo} (°)	γ^d (mN/m)	γ^{nd} (mN/m)	γ (mN/m)
Wetting	98.2 ± 1.8	69.0 ± 2.5	24.5 ± 1.4	1.3 ± 0.2	25.8 ± 1.6
Dewetting	63.1 ± 3.5	60.7 ± 1.3	29.5 ± 0.8	14.8 ± 1.7	44.3 ± 2.5

Table VI Wettability Measurements Performed on PE-1–Treated Silica Surfaces

	θ_{water} (°)	θ_{Diiodo} (°)	γ^d (mN/m)	γ^{nd} (mN/m)	γ (mN/m)
Wetting	81.9 ± 1.5	53.8 ± 0.9	33.7 ± 0.6	4.1 ± 0.4	37.8 ± 1.0
Dewetting	35.0 ± 3.1	33.4 ± 3.8	44.8 ± 1.9	24.0 ± 0.7	68.8 ± 2.6

room temperature using a Spectroscopic Ellipsometer ES 4G from Sopra, with an angle of incidence fixed at 75° with a wavelength λ ranging from 300 to 850 nm. The measurements are taken at intervals of 5 nm. The measured and the fitted curves are analyzed by means of the software Sopra Elli45. All Si/SiO_2 substrates are measured for the first time immediately after the cleaning procedure to determine all their relevant data [n(Si), k(Si), $n(SiO_x)$ and $d(SiO_x)$] by fitting, k being the imaginary part of the refractive index. From the raw data we compute the thickness and the refractive index of the grafted layer without assuming any polymer bulk index as it is usually done with monochromatic ellipsometer. We rather fit the experimental data using the Cauchy's model for the dispersion function of the refractive index:

$$n = A + B/\lambda^2 + C/\lambda^4$$

$$K = D + E/\lambda + F/\lambda^3$$

with initial values being A = 1.5, B = C = D = E = F = 0. We then obtain a curve n(PE) vs. λ reflecting the structure of the thin grafted layer. All the thickness measurements are carried out in air at room temperature (22°C) and normal relative humidity (HR: 50–70%). It should be noted that ellipsometric measurements are macroscopic in nature because the light spot that strikes the surface is $3 \times 6\ mm^2$. The ellipsometric measurement is then an average of the optical properties of the region considered.

The sessile drop method is used to ascertain the presence of a grafted layer and then to characterize its homogeneity and the surface energy of the modified surface. The structure of the grafted layers are analyzed from grafting ratios, ellipsometry measurements (thickness and refractive index) and AFM observations. From the results of these different technics, we will give a general trend of the organization of the grafted layers.

Table VII Contact Angle Hysteresis for the Silica Surfaces with the Various Types of Functionalized Polyethylenes

Polymer Used as Surface Treatment	θ_{water}	θ_{diiodo}
PE-1	46.9 ± 1.6	20.4 ± 2.9
PE-2	35.1 ± 1.7	8.3 ± 1.2
PE-3	10 ± 0.8	8.7 ± 1.5

RESULTS AND DISCUSSION

Precursor Polyethylenes

The characteristics of the polyethylenes are reported in Tables I and II. As expected, the PE-1 polymer synthetized using an homogeneous catalyst displays the lower molar mass compared to the ethylene–hexene copolymer (PE-3). The insertion of the hexene monomer in the PE chain also reduces the crystallinity since the PE-3 is slightly branched. In the present case of grafted polymer monolayers, the crystallinity defined in the bulk state has no significance. Nevertheless, the ability of these PE to crystallize is an important feature for a further cocrystallization with a neat PE matrix.

Silylated Polyethylenes

The functionalization by chlorodimethylsilane performed on the three polymers is evidenced on the infrared spectra. On the FT–IR spectrum of PE3700, it can be seen that the double bond bands of precursor polyethylenes (900, 990, and 1640

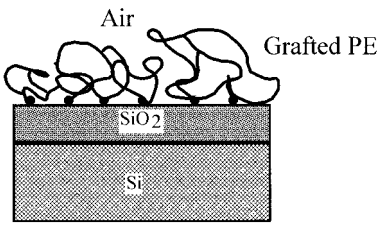

Figure 2 Three-layer model used for ellipsometric data interpretation based on a silicon layer, a native silicon dioxide layer (1.5 nm in thickness), a grafted PE layer and air as medium.

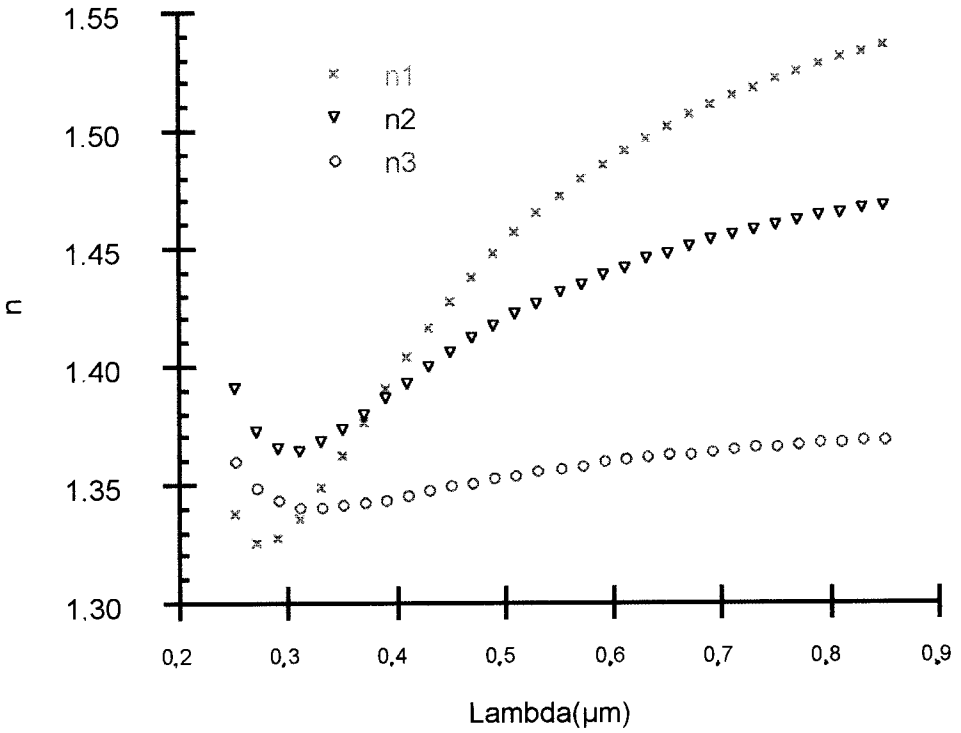

Figure 3 Variation of the refractive index of the grafted layers n_i with wavelength. The curves came from the raw ellipsometric data fitted using a Cauchy's model.

cm^{-1}) have been replaced by the Si—C (800 cm^{-1}) Si—CH_3 (1250 cm^{-1}) or Si—O (1092 cm^{-1}) bands from the silane. The same trend is observed on the other two (Fig. 1).

However, the reaction is not achieved completely. It is very likely that the shorter chains are more functionalized than the longer ones. Hence, the polydispersity of the grafted polymers would be narrower and shifted to lower molecular masses. In any case, we are not able to check it because the GPC analysis is not possible anymore after hydrosylilation.

Grafting

The grafting process can be described by the following reactions:

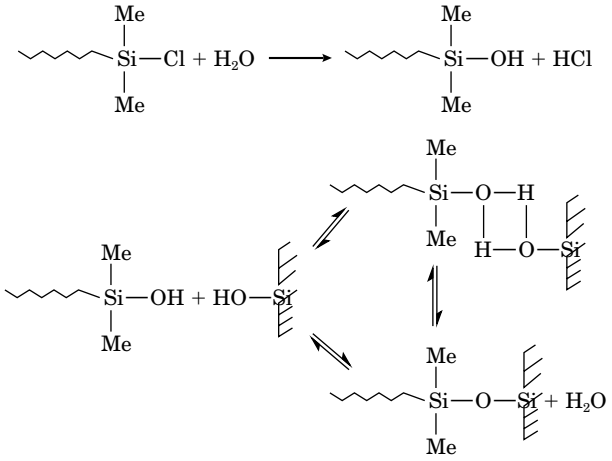

In the first step, the functionalized group of the

Table VIII Grafted-Polymer Thickness h Determined by Ellipsometry, Grafting Ratio Σ from Microanalysis Together with the Distance D between Sites, and Finally the Estimated Radius of Gyration R_g of the Unperturbated Polymer Chain

Polymer	Thickness h (nm)	Grafting Ratio Σ (molecules · nm^2)	$D = 1/\sqrt{\Sigma}$ (nm)	$2R_g$ (nm)
PE-1	5.5	0.02	7.1	1.7
PE-2	4.9	0.01	10	3
PE-3	4	0.001	31.6	6

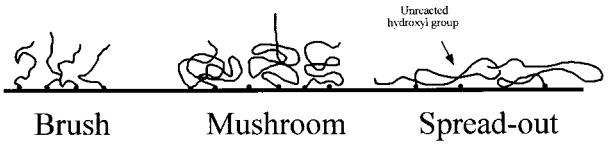

Figure 4 Schematic illustration of the structure of the end-grafted polymer layer.

adsorbed polymer is hydrolyzed by water, which is either already adsorbed on the surface or present in the solvent. In the second step, the adsorbed hydrolyzed polymer via hydrogen bonds reacts with the surface silanol groups to form a siloxane Si—O—Si bond.[30]

The cleaning procedure of the silicon substrate described previously leads to a well-hydrophilic surface. The contact angles measured on such a "clean" surface are less than 10° (the detection threshold of the setup). For comparison, an untreated wafer washed solely by acetone—methanol stirring displays an angle of 45°.

Using probe liquids (Table III), the wettability behavior and the surface energy of the three types of functionalized polymers are determined (Tables IV to VII). As expected, the grafted silicon wafers present a high contact angle, indicating that a layer of chemisorbed polymer is present on the surface. The small standard deviation of values and the invariability of measurements after extensive xylene extractions prove the covalent grafting of polymer chains on the surface. Indeed, a 5-h long soxhlet extraction ensure that physisorbed molecules are removed from the surface. In the case of PE3, three extractions in a row (15 h) do not change the water contact angle at all. It should be remember that because the hydrophobic PE do not establish hydrogen bonds with the hydrophilic surface of silica, the only interaction responsible for physisorbtion are the dispersive van der Waals forces, which is sufficiently weak to be broken; thus, the physisorbed species can be removed easily by a common wash-

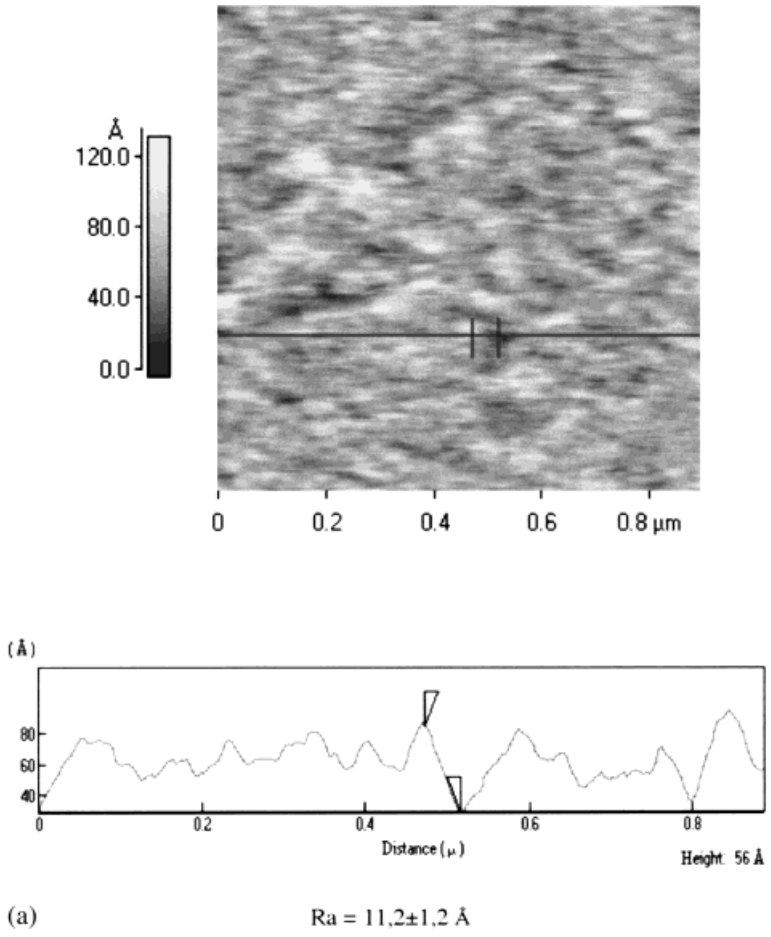

Figure 5 AFM images in air of 0.4 × 0.4 mm^2 area of (a) PE-1-, (b) PE-2-, and (c) PE-3-treated silicon wafers.

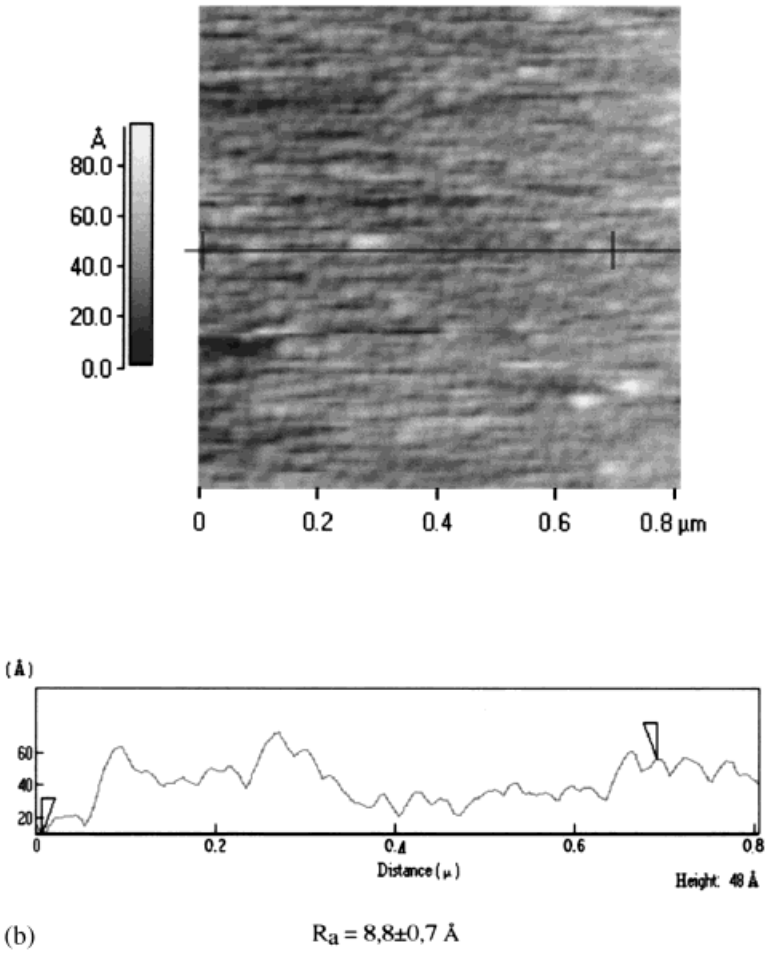

Figure 5 (*Continued from the previous page*)

ing procedure (soxhlet extraction). We observed by wettability experiments that the adsorbtion layer of nonfunctionalized PE on the surface of silica is readily eliminated by a gently cleaning. Moreover, the covalent grafting efficiency is also verified by ^{29}Si NMR on silica particles and by IR Spectroscopic Ellipsometry on silicon wafers.

The contact angle decreases with the molecular mass of the silane-functionalized polymer suggesting a more entangled structure for the PE-3, thus for the longer grafted chain. It should be noted that the contact angle of a neat polyethylene surface is 102°, close to the value of the PE-3.[30] However, if we take into account the dispersive component of the surface energy, it appears that: (a) the surface grafted with PE1 chains is similar to a polyethylene matrix (γ^d = 34,1 mN·m^{-1}); (b) the surfaces grafted with PE2 and PE3 chains display the same behavior as a paraffin surface (γ^d = 26.3 mN·m^{-1}). Moreover, it was shown that an amorphous polymer gives a surface energy lower than a crystalline one.[42] Thus, we can presume that the PE-1 grafting is more ordered than the PE-2 and PE-3. This tendency shows up too in the curves of the refractive index vs. wavelength $n(\lambda)$, which are discussed later (Fig. 3).

Ellipsometric data are analyzed according to a three-layer model previously used in the literature.[33,34] The layers are assumed to be homogeneous and sharp. From the thicknesses obtained it came out that the greater the molecular mass is, the thinner the grafted layer is (Table VIII). It should be noticed that the thicknesses obtained by ellipsometry are corroborated by AFM topographic measurements [see Fig. 5(a)–(c)]. Indeed, for a long chain, the probability for the functionalized group to interact and react with a surface hydroxyl groups is very low. Furthermore, according to its size, the grafted polymer will hinder further grafting by reducing the number of accessible sites (an hydroxyl group occupies 0.22 nm^2 on the surface). Thus, we observe a drop in

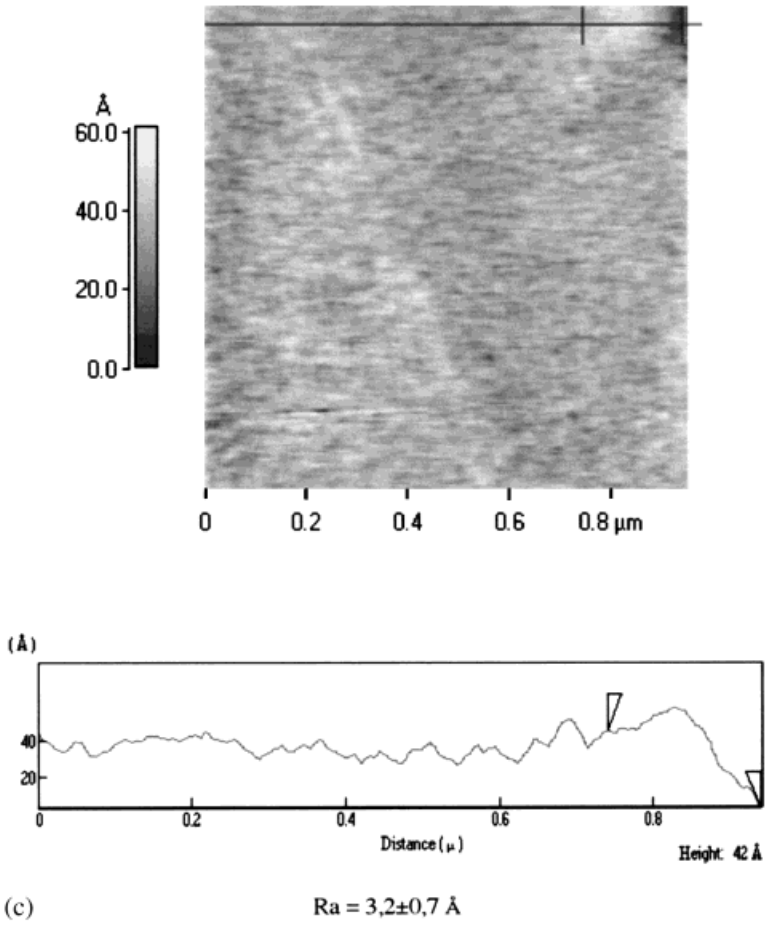

Figure 5 (*Continued from the previous page*)

the grafting density with the polymer molecular weight (see table VIII). Moreover, from the curves n(λ), it appears a peculiar behavior for the refractive index of PE-1 (n_1) compared to other two (Fig. 3). This fact certainly suggests a more structured surface organization.

The thickness of the grafted layer can be compared to the case where the polymer assumes the shape of an "unperturbed" random coil (i.e., the dimensions of the polymer in solution, the unperturbed radius of gyration R_g) (Table VIII). R_g is given by the well-known Flory's relation[35,36]:

$$R_g = 1\sqrt{M/6M_o}$$

where λ, M_o, and M are the effective length and the molar mass of the monomer, and the molar mass of the polymer, respectively. Obviously, in our case, this equation is not longer valid because the polymer is grafted at one chain end.[37] Numerous models were developed to describe the conformations of grafted chains from the characteristics of the chain (number of monomer units, persistence length, etc.) and the grafting density.[33] These models have dealt with so-called wet brushes and cannot be used directly in this case because the thickness is determined for a dry polymer layer.[38] From the correlation between thicknesses, refractive index, grafting ratios (as a consequence the distance between grafted sites, $D = 1/\sqrt{\Sigma}$) and the approximation of the unperturbated radius of gyration, we can estimate the surface conformation[13,39] (Table VIII and Fig. 4). The PE-1 layer is densely grafted forming a pseudo "brush-like" structure, whereas the PE-2 layer displays a "mushroom-like" structure. Finally, the PE-3 polymers are spread out on the surface. Indeed, when the grafting ratio is high (PE1) and D is inferior or equal to the measured thickness the chains tend to fold like mushrooms. Whereas, when the grafting ratio is low and the thickness is small compared to D ($D \gg 2$ h) the chains are isolated and lie on the surface. This view is supported by the distinct variation of n 1.

Furthermore, the comparison between the thickness h and the R_g confirms the brush-like ($h > R_g$), mushroom-like ($h \sim R_g$), and the spread-out ($h < R_g$) structure.

Additionally, from the wetting measurements, it arises that the contact angle hysteresis decreases with increasing the molecular mass of the grafted polymer. The hysteresis can be associated with different phenomena such as the chemical heterogeneity and/or the roughness of the surface, the diffusion of the probe liquid into the sample (or swelling of the substrate), the surface groups reorientation, etc.[37] In most of the cases, the origin of hysteresis is a cooperative effect and it is difficult to quantify each contribution. In this case, we expect that the hysteresis effect is mainly due to the heterogeneous nature of the grafted layer. Indeed, according to the nature of the grafted polymers it is rather impossible to avoid holes in the layer (with smaller molecules like alkylsilane, e.g., it's easier to get a smooth, homogenous monolayer[30]). Thus, the hysteresis is interpreted in terms of the presence of defects in the grafted layer (holes, overthickness). The dependence of the hysteresis angle with the molar mass of the grafted polymer can be considered in addition to the atomic force microscopy analysis[33] [Fig. 5(a) to (c)]. The AFM and the hysteresis of wetting dependencies are in agreement with the ellipsometric measurements, because the PE-3 chains spread out on the silica surface, leading to a smooth and uniform with a low roughness ($R_a = 3.2 \pm 0.7$ Å), hindering the hydroxyl groups and thus decreasing the dewetting hydrophile interactions between water and grafted polymer. Whereas the folded structure of PE-1 leads to a layer displaying a more patchy structure (islands of silica surrounded by a grafted polymer sea). Then, hydrophile interactions between water and appearing hydroxyl sites can be established giving higher hysteresis values. In fact, it can be observed that the PE-3 layer is more uniform than the PE-1 [Fig. 5(a) and (c)]. Holes are more evidenced in the PE-1 layer. The PE-2 displays an intermediate structure. It should be noted that AFM measurements in the z direction (perpendicular to the surface of the specimen) cannot give an absolute value of the thickness of the layer because there is no zero reference. The black areas represent, however, holes with depths varying from 2 nm to 6 nm, assuming the presence of the untreated silica at the bottom of them. Thus, the depth of these holes is in the same range of the thickness determined by ellipsometry. This feature was reported previously in articles devoted to the determination of the thickness of thin films.[40,41]

Thus, the results from wetting measurements, AFM, and ellipsometry are in agreement and lead to the same conclusions on the presence and the structure of the polyethylenes covalently bonded on a silica surface.

CONCLUSIONS

The grafting efficiency of chlorosilane-terminated polyethylenes on silica surfaces is demonstrated by using ^{29}Si NMR and wetting measurements. In fact, the large differences in the surface properties of the grafted chains and the substrate allow us to check the presence of chemically attached polymer chains on the surface. The values of the dry layer thicknesses determined by ellipsometry and the radius of gyration of the unperturbated chains for the different molar masses of the functionalized polymer are compared, keeping in mind the grafting ratios determined by microanalysis and a general trend in the surface organization of the tethered chains is then proposed. For the lower molar mass, the polymer chains display a pseudobrush-like conformation and for the highest molar mass the polymer chains are spread out on the surface. As a consequence, as evidenced by atomic force microscopy, the layers prepared from the lower molar mass silane-functionalized polyethylene displays holes, whereas the high molar mass PE ones display a more homogeneous surface. These observations are confirmed by the dependence of the wetting hysteresis with the molar mass of the grafted chains.

This work was done under the financial support of the M.R.E.S Ministry. The authors would thank Dr. D. Sage for developing wetting measurements and N. Verdel for preparing the polymers.

REFERENCES

1. J. F. Gerard and B. Chabert, *Macromol. Symp.,* **108,** 137 (1996).
2. J. L. Thomason and A. A. Van Rooyen, *J. Mater. Sci.,* **27,** 5 (1992).
3. D. Campbell and M. M. Qayyun, *J. Polym. Sci., Polym. Phys. Ed.,* **18,** 83 (1980).
4. R. H. Burton and J. M. Folkes, *Plast. Rubber Process. Appl.,* **3,** 129 (1983).
5. B. S. Hsiao and E. J. H. Chen, in *Controlled Interphases in Composite Materials,* H. Ishida, Ed., Elsevier, New York, 1990, p. 613.

6. J. I. Lauritzen and J. D. Hoffman, *J. Appl. Phys.,* **44,** 4370 (1973).
7. H. Ishida and P. Bussi, *Macromolecules,* **24,** 3569 (1991).
8. G. P. Desio and L. Rebenfeld, *J. Appl. Polym. Sci.,* **39,** 825 (1990).
9. E. Devaux and B. Chabert, *Polym. Commun.,* **32,** 464 (1991).
10. J. Varga and J. Karger–Kocsis, *Polym. Bull.,* **30,** 105 (1993).
11. F. Hoecker and J. Karger–Kocsis, *Polym. Bull.,* **31,** 707 (1993).
12. J. L. Thomason and A. A. Van Rooyen, *J. Mater. Sci.,* **27,** 897 (1992).
13. A. Halperin, M. Tirrell, and T. P. Lodge, *Adv. Polym. Sci.,* **31,** 100 (1992).
14. P. G. de Gennes, *J. Physiol. (Paris),* **37,** 1443 (1976).
15. T. Cosgrove, T. G. Heath, J. S. Phipps, and R. M. Richardson, *Macromolecules,* **24,** 94 (1991).
16. P. Auroy, L. Auvray, and L. Leger, *Phys. Rev. Lett.,* **66,** 719 (1991).
17. H. R. Brown, *Annu. Rev. Mater. Sci.,* **21,** 463 (1991).
18. H. R. Brown, V. R. Deline, and P. F. Green, *Nature,* **341,** 221 (1989).
19. C. Creton, E. J. Kramer, C. Y. Hui, and H. R. Brown, *Macromolecules,* **25,** 3075 (1992).
20. H. R. Brown, K. Char, V. R. Deline, and P. F. Green, *Macromolecules,* **26,** 4155 (1993).
21. J. F. Feller, B. Chabert, R. Spitz, A. Guyot, and J. F. Gerard, *Compos. Interfaces,* **3,** 121 (1995).
22. J. F. Feller, B. Chabert, R. Spitz, A. Guyot, H. D. Wagner, and J. F. Gerard, *J. Adhes.,* **58,** 299 (1996).
23. J. F. Gerard, B. Chabert, A. Guyot, R. Spitz, *PMSE-ACS Preprints,* **75,** 480 (1996).
24. L. Gonon, A. Momtaz, D. Van Hoywegaen, B. Chabert, J. F. Gerard, and R. Gaertner, *Polym. Compos.,* **17,** 265 (1996).
25. L. Gonon, B. Chabert, A. Bernard, D. Van Hoywegden, and J. F. Gerard, *J. Adhes.,* to appear.
26. L. Gonon, PhD Thesis, Univ. of Lyon (1995).
27. E. Boucher, J. P. Folkers, H. Hervet, L. Leger, and C. Creton, *Macromolecules,* **29,** 774 (1996).
28. J. Duchet, B. Chabert, J. P. Chapel, J. F. Gerard, J. M. Chovelon, and N. Jaffrezic–Renault, *Langmuir,* to appear.
29. J. Duchet, J. P. Chapel, B. Chabert, and J. F. Gerard, *Polymer Preprints,* **37,** 88 (1996).
30. J. Duchet, J. P. Chapel, B. Chabert, and J. F. Gerard, *Macromolecules,* to appear.
31. F. M. Fowkes, *Ind. Eng. Chem.,* **12,** 40 (1964).
32. R. M. A. Azzam and N. M. Bashara, in *Ellipsometry and Polarized Light,*, North Holland, Amsterdam, 1992.
33. D. F. Siqueira, U. Breiner, R. Stadler, and M. Stamm, *Langmuir,* **11,** 1680 (1995).
34. F. L. McCrackin, E. Passaglia, R. R. Stromberg, and H. L. Steinberg, *J. Res. Natl. Bur. Std.,* **67A,** 363 (1963).
35. P. J. Flory, in *Principles of Polymer Chemistry,*, Cornell Univ. Press, Ithaca, NY, 1953.
36. P. J. Flory, in *Statistical Mechanics of Chain Molecules,* J. Wiley, New York, 1959.
37. J. Israelachvili, in *Intermolecular & Surface Forces,* Academic Press, New York, 1992.
38. S. T. Milner, *Science,* **251,** 905 (1991).
39. G. J. Fleer, M. A. C. Stuart, J. M. H. M. Ssheutjens, T. Cosgrove, and B. Vincnet, in *Polymers at Interfaces,* Chapmann and Hall, London, 1993.
40. S. Biggs and F. Grieser, *J. Colloid Interface Sci.,* **165,** 425 (1994).
41. M. Fujii, S. Sugisawa, K. Fukada, T. Kato, T. Shirakawa, and T. Seimiya, *Langmuir,* **10,** 984 (1994).
42. S. Wu, in *Polymer Interface and Adhesion,* Marcel Dekker, Inc., New York, 1982.